

# Spectral resolution of light field spectral imaging system under diffraction model



Hu Liang<sup>a</sup>, Yuan Yan<sup>a,\*</sup>, Su Lijuan<sup>a</sup>, Huang Min<sup>b</sup>, Li Yang<sup>b</sup>

<sup>a</sup> Beihang University, Key Laboratory of Precision Opto-mechatronics Technology of Ministry of Education, Xueyuan Road No.37, Haidian District, Beijing, 100191, China

<sup>b</sup> Academy of Opto-Electronic, Chinese Academy of Science, Beijing 100094, China

## ARTICLE INFO

### Keywords:

Light field  
Imaging spectrometer  
Diffraction model  
Spectral resolution

## ABSTRACT

A light field camera has a powerful and unique capability of light-ray collection and post-processing of data. In this paper, we describe a micro-lens-array-based approach to acquire the light field, with the added utility provided by simultaneous placement of linear variable filters (LVF) directly in the camera's pupil plane. The new imaging spectrometer is capable of collecting the spectral segment information in the entire spectral range through only one exposure. Owing to the potential application of spectral detection, interest in the spectrum detection ability of the system is on the rise. As pixel sizes are reduced, consideration of diffraction effects in the system becomes increasingly important. We discuss a light field spectral imaging system and its wave propagation analysis. Then, we simulate a system response using our diffraction model and discuss the spectral resolution calibration with the application of the system model. In addition, the spectral resolution of the light field spectral imaging system is tested using the monochromator method; the results are found to be in good agreement with the simulation results.

© 2017 Elsevier B.V. All rights reserved.

## 1. Introduction

Light field imaging has the unique ability to develop a conventional imaging system to record four-dimensional (4D) information in a single frame, including two-dimensional (2D) spatial and angular information [1]. By utilising light field imaging systems, various applications, such as multi-angle imaging, depth imaging, refocusing and multi-modal imaging, are developed [2–5]. R. Horstmeyer et al. used an array of filters to divide the objective aperture of a light field structure for modulating a spectrum polarisation state in a single exposure. However, the design utilised a pinhole-lens array that offers less optical efficiency and worse resolution [5,6]. Zhou et al. proposed another design using a micro-lens array [7]. In this paper, a linear variable filter (LVF) array was assembled into the light field camera instead of an array of filters, capturing a greater number of spectral bands.

In this paper, the main purpose is to evaluate the spectral detecting performance of a light field spectral imaging system using a wave optics approach. This paper begins with a brief discussion on the general concept of a light field camera. A more detailed explanation of similar light field set-ups is available in Fig. 1. A micro-lens array (MLA), positioned in the traditional image plane, re-images the pupil of the

main lens at the sensor. This configuration allows the cone of rays from a single point in object space to focus at each micro-lens, propagate beyond the plane of the micro-lens, spread out, and be sampled with multiple pixels. The rays enter the main lens, filter array, and MLA. During transmission, the diffraction of the system causes the image to become blurred, leading to lower spectral precision.

## 2. Imaging system simulation

In this study, a numerical simulation of light propagating in a light field imaging system has been performed using a wave optics approach [8–11]. For simplicity, in the simulation analysis, the main lens is considered as a single thin lens. The imaging system is considered to be incoherent. In addition, the objective is assumed to be an ideal point source. Fig. 2 is a schematic layout of such a system. The spatial coordinates of the object plane are denoted by  $(\xi, \eta)$ . The coordinates of the main lens are denoted by  $(x, y)$ , and the distance from the object to the main lens is  $Z_1$ . The coordinates of the micro-lens array are denoted by  $(u, v)$ , and the distance from the main lens to the micro-lens array is  $Z_2$ . The coordinates of the sensor are denoted by  $(t, w)$ , and the distance

\* Corresponding author.

E-mail addresses: [lianfengge@163.com](mailto:lianfengge@163.com) (H. Liang), [yuanyan@buaa.edu.cn](mailto:yuanyan@buaa.edu.cn) (Y. Yan).

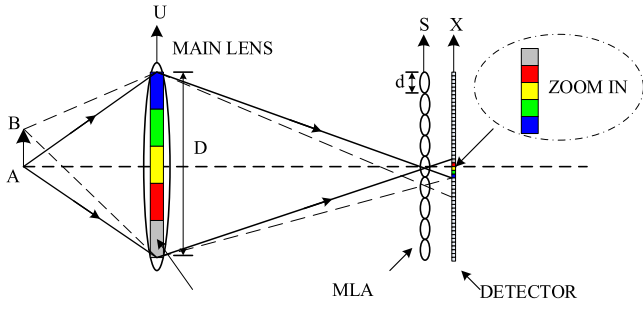


Fig. 1. Schematic of the principle of a light field spectral imaging system.

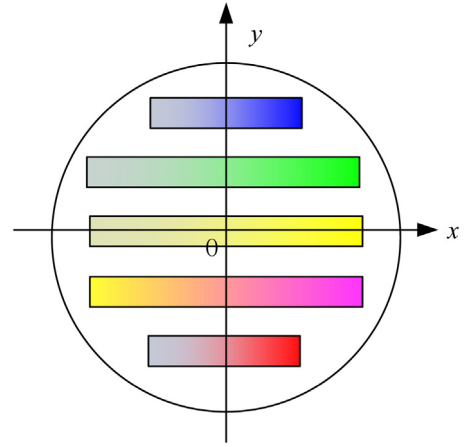


Fig. 3. The arrangement of the filter array.

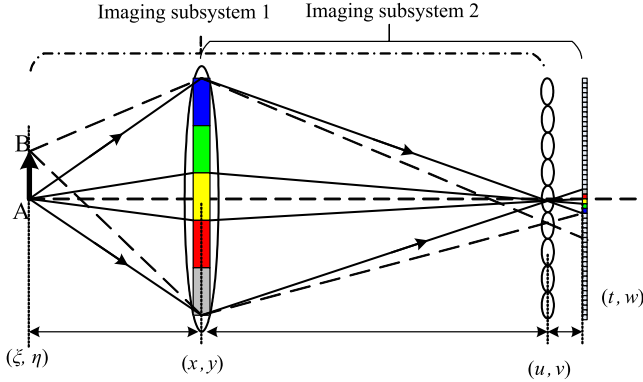


Fig. 2. Schematic layout of a light field spectral imaging system, with the first subsystem containing the main lens and the LVF array, and the second subsystem containing the micro-lens array and the detector.

from the micro-lens array to the sensor is  $Z_3$ . The focal lengths of the main lens and the micro-lens array are  $f_1$  and  $f_2$ , respectively. The diameter of the main lens is  $D$ , while that of the micro-lens is  $d$ .

In order to analyse this optical layout and the light collected at the sensor, we perform a wave analysis from one plane to another. First, assuming that the laser point source,  $\delta$ , in the object plane,  $(\xi, \eta)$ , we denote the generalised pupil function for the main lens by  $U_1$ , and its impulse response is

$$U_1(x, y) = \frac{1}{j\lambda z_1} \exp \left\{ j \frac{k}{2z_1} [(x - \xi)^2 + (y - \eta)^2] \right\}. \quad (1)$$

The filter array is placed at the main lens plane, thus, the generalised pupil function,  $U_2$ , passing through the main lens, the filter array and the field is

$$U_2(x, y) = U_1(x, y) P(x, y) \exp \left\{ j \frac{k}{2f_1} [x^2 + y^2] \right\}. \quad (2)$$

In Eq. (2),  $P(x, y)$  is the pupil function of the filter array [12]. The arrangement of the filter is shown in Fig. 3. The representation of the pupil function of the array related to the arrangement of the filter is

$$P(x, y) = \begin{cases} \tau(\lambda)_{(x,y)} & \sqrt{x^2 + y^2} \leq \frac{D}{2} \\ 0 & \sqrt{x^2 + y^2} > \frac{D}{2}. \end{cases} \quad (3)$$

In Eq. (3),  $\tau(\lambda)_{(x,y)}$  is the transmissivity function of wavelength,  $\lambda$ , at the position,  $(x, y)$ .

In Fig. 3, each band is an LVF, whose wavelength changes linearly along the  $x$ -direction; at the position  $(x, y)$ , the energy distribution is approximated as a Gaussian distribution. Assuming  $\lambda_0$  is the centre wavelength at  $(x_0, y_0)$ , when the incident wavelength is  $\lambda_i$ , the response function at  $(x_0, y_0)$  is simplified as [13]

$$\tau(\lambda_i) = A(\lambda_0) e^{-\frac{(\lambda_i - \lambda_0)^2}{\sigma^2(\lambda_0)}}, (x_0, y_0) \rightarrow \lambda_0. \quad (4)$$

In Eq. (4),  $A(\lambda_0)$  is denoted as the maximum transmission rate at the wavelength,  $\lambda_0$ .

In the same manner, the complex amplitude distribution of the laser impulse response, denoted as  $h_1(u, v, \xi, \eta)$  at the micro-lens array plane, is derived as

$$h_1(u, v, \xi, \eta) = \frac{1}{j\lambda z_2} \int \int_{-\infty}^{\infty} U_2(x, y) \times \exp \left\{ j \frac{k}{2z_2} [(x - u)^2 + (v - y)^2] \right\} dx dy. \quad (5)$$

Similarly, the micro-lens array could also be viewed as a sampling function, and its representation is

$$M(u, v) = \begin{cases} 1 & \sqrt{u^2 + v^2} \leq \frac{D_2}{2} \\ 0 & \sqrt{u^2 + v^2} > \frac{D_2}{2}. \end{cases} \quad (6)$$

According to Eqs. (5) and (6), the field distribution of the target, which passes through the main lens, filter array and micro-lens array, is derived as

$$U_3(u, v) = h_1(u, v) \sum_m \sum_n M(u - mD_2, v - nD_2) \times \exp \left\{ j \frac{k}{2f_2} [(u - mD_2)^2 + (v - nD_2)^2] \right\}. \quad (7)$$

The power of the impulse function,  $\delta$ , passes through the main lens, filter array and the micro-lens array. Finally, the field propagates to the sensor at a distance,  $z_3$ , and denoted as  $h(t, w)$ . The intensity captured by the sensor is,

$$h(t, w) = \frac{1}{j\lambda z_3} \int \int_{-\infty}^{\infty} U_3(u, v) \times \exp \left\{ j \frac{k}{2z_3} [(t - u)^2 + (w - v)^2] \right\} dudv. \quad (8)$$

The spectral radiance distribution in the LVFs is not infinitely narrow. In addition, existing film coating technology is not perfect, which causes a difference in the spectral properties between the real and ideal LVF. The deviation occurs at the position of the middle-wavelength, spectral resolution, etc.

In the light field spectral imaging system used for experiment, the LVF is projected onto the sensor plane. Fig. 4 shows the corresponding relationship between the response width,  $L$ , and the size of a pixel. In light of this, the spectral resolution of the imaging system is determined by the splitting property of the LVF, size of the pixel,  $s$ , and how the diffraction is affected by the system.

$$L = L_2 - L_1 = \frac{f_1}{f_2} s. \quad (9)$$

Download English Version:

<https://daneshyari.com/en/article/5449163>

Download Persian Version:

<https://daneshyari.com/article/5449163>

[Daneshyari.com](https://daneshyari.com)